REFERENCES

An-Hui, L., Dongyuan, Z., and Ying, W. (2010) Nanocasting: A versatile strategy for creating nanostructured porous materials. Advanced Materials, 18(14), 1793-1805.

Avgouropoulos, G., Ioannides, T., Papadopoulou, C., Batista, J., Hocevar, S., and Matralis, H.K. (2002) A comparative study of Pt/g-Al_2O_3, Au/a-Fe_2O_3 and CuO-CeO_2 catalysts for the selective oxidation of carbon monoxide in excess hydrogen. Catalysis Today, 75, 157-167.

Ayastuy, J.L., Gurbani, A., Gonzalez-Marcos, M.P., and Gutierrez-Ortiz, M.A. (2010) Effect of copper loading on copper-ceria catalysts performance in CO selective oxidation for fuel cell applications. International Journal of Hydrogen Energy, 35, 1232-1244.

Bond, G.C., and Thompson, D.T. (1999). Catalysis by Gold. Catalysis Reviews: Science and Engineering, 41(3-4), 319-388.

Candusso, D., Harel, F., Bernardinis, A.D., Francois, X., Pera, M.C., Hissel, D., Schott, P., and Coquery, G. (2006) Characterisation and modelling of a 5 kW PEMFC for transportation applications. International Journal of Hydrogen Energy, 31, 1019-1030.

Deeprasertkul, C., Longloilert, R., Chaisuwan, T., and Wongkasemjit, S. (2015) Impressive low reduction temperature of synthesized mesoporous ceria via nanocasting. Materials Letters, 130, 218-222.

Echigo, M., and Tabata, T. (2003) A study of CO removal on an activated Ru catalyst for polymer electrolyte fuel cell applications. Applied Catalysis A: General, 251(1), 157-166.

Fan, H., Lopez, G.P., Brinker, C.J., and Lu, Y. (2002) U.S. Patent 6 471 761.

Gamboa-Rosales, N.K., Ayastuy, J.L., Gonzalez-Marcos, M.P., and Gutierrez-Ortiz, M.A. (2011) Effect of Au promoter in CuO/CeO_2 catalysts for the oxygen-assisted WGS reaction. Catalysis Today, 176, 63-71.

Gamboa-Rosales, N.K., Ayastuy, J.L., Gonzalez-Marcos, M.P., and Gutierrez-Ortiz, M.A. (2012) Oxygen-enhanced water gas shift over ceria-supported Au-Cu bimetallic catalysts prepared by wet impregnation and deposition-precipitation. International Journal of Hydrogen Energy, 37, 7005-7016.

Gorte, R.J. and Zhao, S. (2005) Studies of the water-gas-shift reaction with ceria-supported precious metals. Catalysis Today, 104, 18-24.

Haruta, M., Tsubota, S., Kobayashi, T., Kageyama, H., Genet, M.J., and Delmon, B. (1993) Low-temperature oxidation of CO over gold supported on TiO_2, alpha-Fe_2O_3, and Co_3O_4. Journal of Catalysis, 144(1), 175-192.

Hu, Y., Dong, L., Shen, M., Liu, D., Wanf, J., and Ding, W. (2001) Influence of support on the activities of copper oxide species in the low-temperature NO-CO reaction. Applied Catalysis B: Environment, 31(1), 61-69.

Idakiev, V.,Tabakova, T.,Naydenov, A.,Yuan, Z.-Y., and Su, B.-L. (2006) Gold catalysts supported on mesoporous zirconia for low-temperature water-gas shift reaction. Applied Catalysis B, 63, 178-186.

Ji, P., Zhang, J., Chen, F., and Anpo, M. (2008) Ordered mesoporous CeO_2 synthesized by nanocasting from cubic Ia3d mesoporous MCM-48 silica: formation, characterization and photocatalytic activity. The Journal of Physical Chemistry C, 112, 17809-17813.

Kresge, C.T., Leonowicz, M.E., Roth, W.J., Vartuli, J.C., and Beck, J.S. (1992) Ordered mesoporous molecular sieves synthesized by a liquid-crystal template mechanism. Letters to Nature, 359, 710-712.

Lee, S.J., and Gavriilidis, A. (2002) Supported Au catalysts for low-temperature CO oxidation prepared by impregnation. Journal of Catalysis, 206(2), 305-313.

Liu, W. and Flytzani-Stephanopoulos, M. (1995) Total Oxidation of Carbon Monoxide and Methane over Transition Metal Fluorite Oxide Composite Catalysts: I. Catalyst Composition and Activity. Journal of Catalysis, 153(2), 304-316.

Longloilert, R., Chaisuwan, T., Luengnaruemitchai, A., and Wongkasemjit, S. (2011) Synthesis of MCM-48 from Silatrane via sol-gel process. Journal of Sol-Gel Science and Technology, 58, 427-435.

Monnier, A., Schuth, F., Huo, Q., Kumar, D., Margolese, D., Maxwell, R.S., Stucky, M., Krishnamurty, G.D., Petroff, P., Firouzi, A., and Janicke, M. (1993) Cooperative formation of inorganic-organic interfaces in the synthesis of silicate mesostructures. Science, 261, 1299-1303.

Ou, T.C., Chang, F.W., and Roselin, L.S. (2008) Production of hydrogen via partial oxidation of methanol over bimetallic Au-Cu/TiO_2 catalysts. Journal of Molecular Catalysis A: Chemical, 293(1-2), 8-16.

Phiriyawirut, P., Magaraphan, R., Jamieson, A.M., and Wongkasemjit, S. (2003) Morphology study of MFI Zeolite synthesized directly from Silatrane and Alumatrane via the sol-gel process and microwave heating. Microporous Mesoporous Mater, 64(1-3), 83-93.

Pintar, A., Batista, J., and Hocevar, S. (2005) TPR, TPO, and TPD examinations of $Cu_{0.15}Ce_{0.85}O_{2-y}$ mixed oxides prepared by co-precipitation, by the sol-gel peroxide route, and by citric acid-assisted synthesis. Journal of Colloid and Interface Science, 285(1), 218-231.

Praliaud, H., Mikhailenko, S., Chajar, Z., and Primet, M. (1998) Surface and bulk properties of Cu-ZSM-5 and Cu/Al_2O_3 solids during redox treatments. Correlation with the selective reduction of nitric oxide by hydrocarbons. Applied Catalysis B: Environment, 16(4), 359-374.

St-Pierre, J. and Wilkinson, D. (2001) Fuel cells: a new, efficient and cleaner power source. American Institute of Chemical Engineers Journal, 47(7), 1482-1486.

Trovarelli, A., Leitenburg, C.D., Boaro, M., and Dolcetti, G. (1999) The utilization of ceria in industrial catalysis. Catalysis Today, 50(2), 353-367.

Wang, J., Lin, S., and Huang, T. (2002) Selective COad oxidation in rich hydrogen over CuO/samaria-doped ceria. Applied Catalysis A: General, 232(1-2), 107-120.

Xu, J., Luan, Z., He, H., Zhou, W., and Kevan, L. (1998) A reliable synthesis of cubic mesoporous MCM-48 molecular sieve. Chemistry of Materials, 10(11), 3690-3698.

APPENDIX

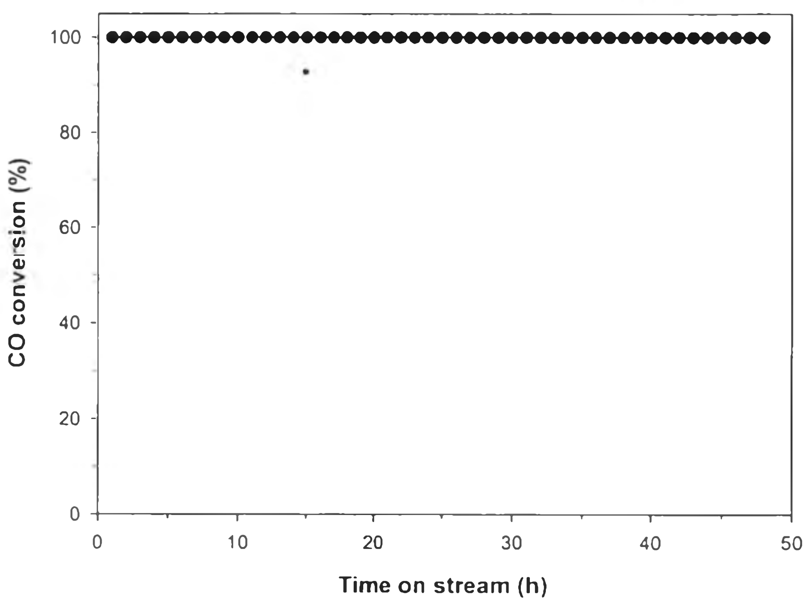

Figure A1 Effect of time on stream on the stability of $7CuO/CeO_2$ under PROX reaction.

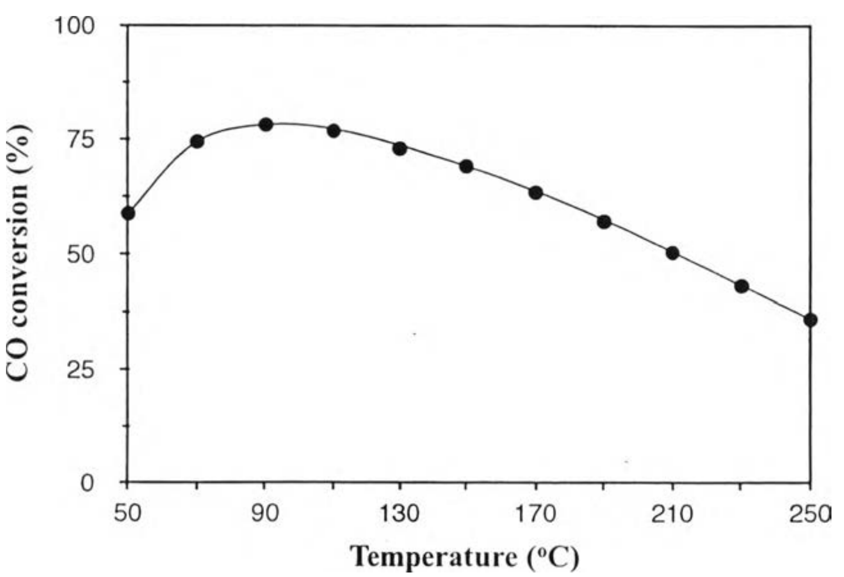

Figure A2 CO conversion of $1Au/CeO_2$ for PROX reaction using feed composition of 1%CO, 1%O_2, 40%H_2 balance in He.

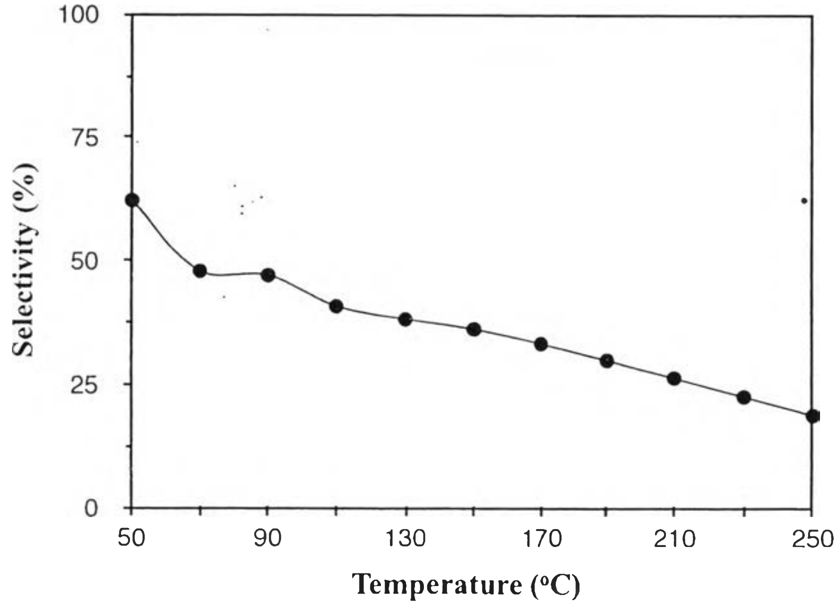

Figure A3 Selectivity of 1Au/CeO_2 for PROX reaction using feed composition of 1%CO, 1%O_2, 40%H_2 balance in He.

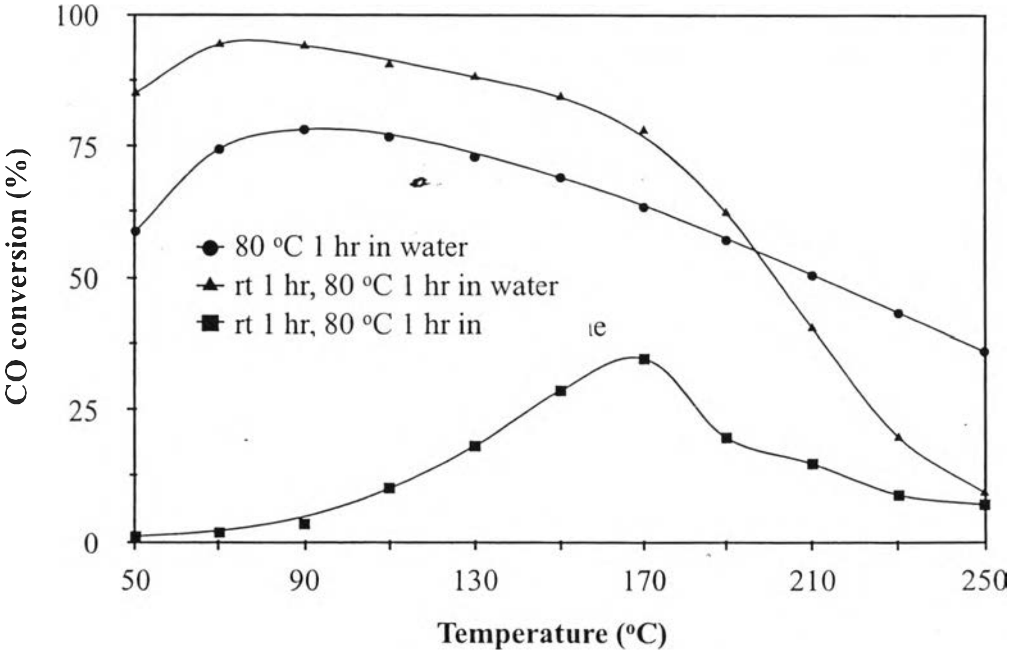

Figure A4 CO conversion of 1Au/CeO_2 with different step of DP method for PROX reaction.

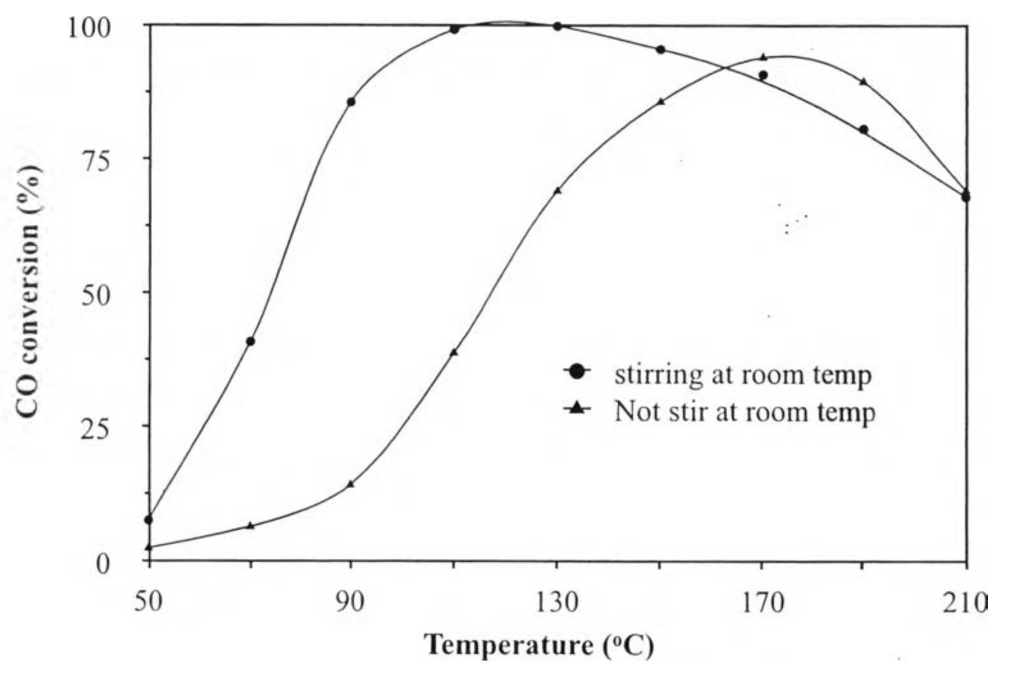

Figure A5 CO conversion of $7CuO/CeO_2$ with different step of DP method for PROX reaction.

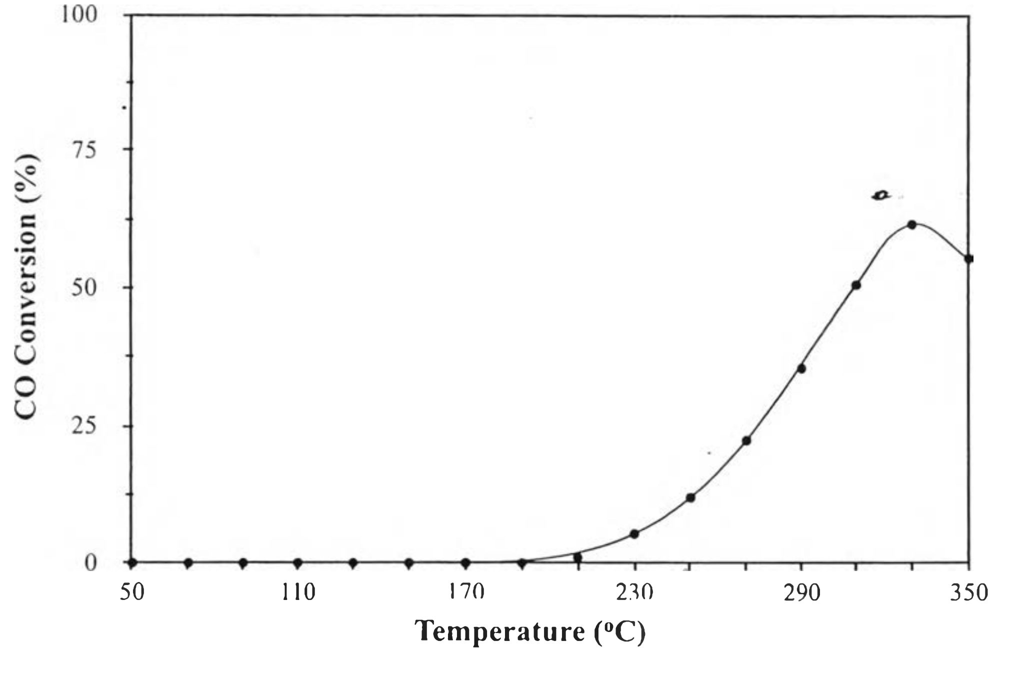

Figure A6 CO conversion of pure MSP ceria for PROX reaction using feed composition of 1%CO, 1%O_2, 40%H_2 balance in He.

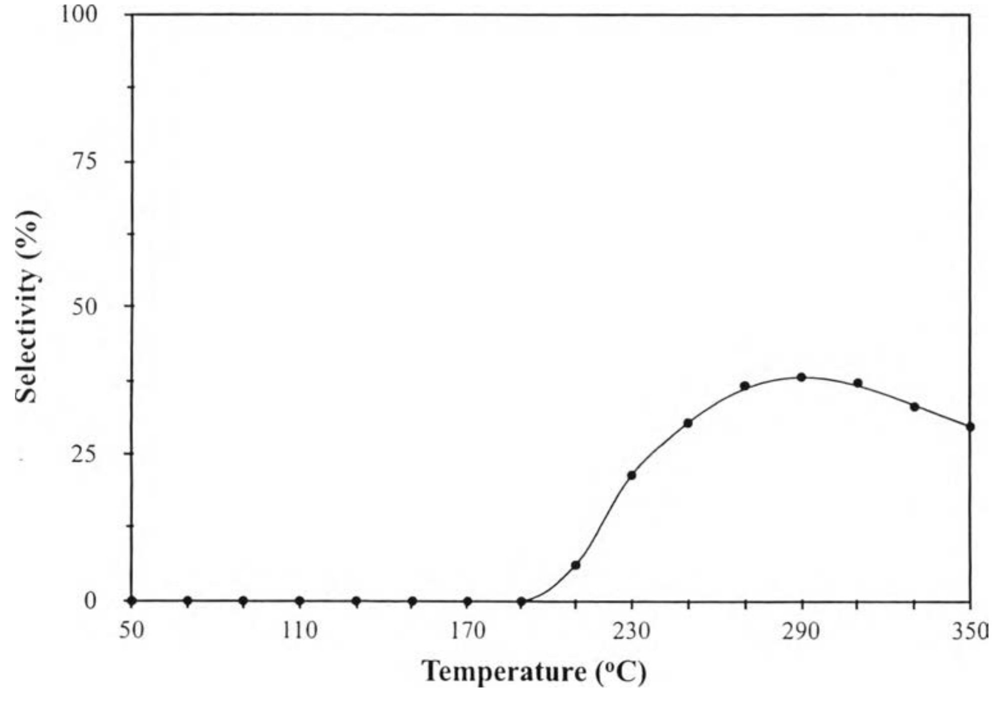

Figure A7 Selectivity of pure MSP ceria for PROX reaction using feed composition of 1%CO, 1%O_2, 40%H_2 balance in He.

Calculation A1 Scherrer's equation.

$$L = \frac{K\lambda}{\beta.\cos\theta}$$

where L = the average crystallite size

λ = the X-ray wavelength in nanometer (nm)

β = the peak width of the diffraction peak profile at half maximum height in radians

K = constant related to crystallite shape; spherical crystals with cubic symmetry is 0.94

θ = the diffraction peak position

Example: Calculate the average crystallite size of pure MSP ceria from the diffraction peak at 2θ = 28.5479°, β= 2.2819° by using the X-ray wavelength at 0.15406 nm

First: Convert β from degrees to radians

β = 0.0398 radians

Second: Calculate cosθ from the diffraction peak at 2θ = 28.5479° (the θ can be in degrees or radians, since the cosθ corresponds to the same number)

Final: Using above equation to determine the average crystallite size

$$L = \frac{0.94 \times 0.15406 nm}{0.0398 radius \times \cos(14.2740^{o})} = 3.750 nm$$

Calculation A2 Lattice parameter by considering as a cubic crystal.

$$\frac{1}{d^2} = \frac{h^2 + k^2 + l^2}{a^2}$$

where d = d-spacing

h,k,l = plane (h,k,l)

a = cell parameter

Example: Calculate the lattice parameter from a plane (1,1,1) which has a spacing between this plane of 3.1244 $\mathring{A}$

$$\frac{1}{3.1244^2} = \frac{1^2 + 1^2 + 1^2}{a^2}$$

$$a = 5.4116 \quad \mathring{A}$$

Calculation A3 calculation of the amount of Ce^{3+} (%) on the surfaces of ceria based catalysts.

$$Ce^{3+}(\%) = \frac{S(Ce^{3+})}{S(Ce^{3+} + Ce^{4+})} \times 100$$

where $S(Ce^{3+}) = v^o + u^o + v' + u'$

$S(Ce^{4+}) = v + u + v' + u' + v'' + u''$

Example: Calculate the amount of Ce^{3+} (%) on the surfaces of pure MSP ceria

$S(Ce^{3+})$ = 5.4+10.3+11.3+15.7 = 42.7

$S(Ce^{4+})$ = 9.2+5.4+10.3+18.4+11.3+15.7 = 70.3

$$Ce^{3+}(\%) = \frac{42.7}{70.3 + 42.7} \times 100 = 37.8$$

Calculation A4 Kubelka-Munk function.

$$f(r) = \frac{(1-r)^2}{2r}$$

where f(r) = Kubelka-Munk function

r = reflectance fraction

Example: Convert the reflectance(%) of 47.0 (at the wavelength of 200 nm) to the absorbance

First: Convert reflectance(%) into fraction

$$\text{reflectance(fraction)} = \frac{47.0}{100} = 0.47$$

Second: Convert the reflectance into absorbance

$$f(r) = \frac{(1-0.47)^2}{2 \times 0.47} = 0.30$$

CURRICULUM VITAE

Name: Mr. Kanapos Wangkawee

Date of Birth: March 28, 1991

Nationality: Thai

University Education:

2009-2012 Bachelor Degree of Science in Chemistry, Faculty of Science, Chiang Mai University, Chiang Mai, Thailand.

Publications

1. Wangkawee, W.; Laongnuan, S.; and Nimmanpipug P. (2014) Investigation of Vibrational Properties and Ferroelectric Instability of Doped Perovskite Barium Titanate ($BaTi_{0.6}Nb_{0.2}Fe_{0.1}O_3$)", Ferroelectrics, 458(1): 122-126.

Presentations:

1. Wangkawee, W.; Laongnuan, S.; Nimmanpipug P. (2012, December 9-14) Investigation of Vibrational Properties and Ferroelectric Instability of Doped Perovskite Barium Titanate ($BaTi_{0.6}Nb_{0.2}Fe_{0.1}O_3$), Paper presented at the 8^{th} Asian Meeting on Ferroelectrics (AMF-8), Pattaya, Thailand.